Model for the Evolution of Dislocation Loops in Silicon

Ibrahim Avci, [1] Hernan A. Rueda[2], Mark E. Law[1]

1. University of Florida Swamp Center Room 538
New Engineering Building PO Box 116130
Gainesville FL 32611

2. Motorola Inc
2100 East Elliot Road
Tempe AZ 85284

Abstract-A single statistical point defect based model for the evolution of dislocation loops during oxidation and annealing under an inert ambient is developed. The model assumes that the radius and the density of the dislocation loops follow a log normal distribution. The capture or emission rate of interstitials bounded by the dislocation is proportional to the rates of emission and absorption of point defects at the loop boundaries modulated by a log normal loop distribution function. The model incorporates the stress due to dislocation loops as well. The published data on loop evolution and distribution under oxidation and inert ambient annealing conditions are used to calibrate the loop model.

INTRODUCTION

High dose ion implantation is one of many process steps used in process technologies today. If the dose is high enough, it results in the formation of an amorphous layer of Si and produces large amount of extended defects below the amorphous/crystalline (a/c) interface [1]. In order to activate dopants and repair the implantation damage, annealing is required. Upon annealing, the amorphous region re-grows through solid phase epitaxy (SPE) with end-of-range (EOR) dislocation loops [2] formed at the (a/c) interface.

Dislocation loops affect the device performance in three main ways. First, they significantly increase leakage current when located in the depletion layer of a junction [3]. Second, they indirectly affect the dopant re-distribution by capturing and emitting point defects [4]. Third, diffusion of dopant- defect complexes and clusters may be affected due to stress generated by dislocation loops. Different non-equilibrium processes (e.g., oxidation) affect the loop growth and the loop dissolution in different ways. Oxidation injects interstitials [5] into the bulk and these interstitials contribute to the growth of dislocation loops. During annealing under an inert ambient, loop-to-loop interaction becomes more dominant and the large loops grow at the expense of smaller ones [6] (Ostwald ripening).

This paper explains a single statistical point defect based model for the evolution of dislocation loops during oxidation and annealing under an inert ambient. First, we explain the model and then give the simulation results for various experiments.

MODELING

The model is based on the assumption that the radius and the density of the dislocation loops follow a log normal distribution (LND). LND is continuous distribution in which the logarithm of a variable has a normal distribution. The unnormalized probability distribution function $f_D(R)$ is represented as:

$$f_D(R) = \frac{Dall}{SR\sqrt{2\pi}} e^{-(\ln(R)-M)^2/(2S^2)} \quad (1)$$

where R is the loop radius, and Dall (cm^{-3}) is total density of the loops. S and M are the deviation and the mean of LND. M and S can be derived from Gaussian parameters, deviation (σ) and mean (μ), as follows:

$$\mu = e^{M+S^2/2}, \ \sigma^2 = e^{S^2+2M}(e^{S^2}-1) \quad (2)$$

Total density of interstitials bounded by the loops, Nall(cm^{-3}), can be calculated using probability distribution function and the atomic density of Si atoms on the (111) plane (n_a=1.5e15 cm^{-2}).

$$Nall = \int_0^\infty \pi R^2 n_a f_D(R) dR \quad (3)$$

$$Nall = Dall \pi n_a e^{(2S^2+2M)}$$

Loops primarily affect the equilibrium concentration of point defects around the loop layer [7]. The effective local equilibrium concentration of interstitals (C_{Ib}) and vacancies (C_{Vb}) at the loop layer boundaries are the following [8,9]:

$$C_{Ib} = g_{bc} C_I^*(P) e^{-(\frac{\Delta E_f}{kT})} \quad (4)$$

$$C_{Vb} = g_{bc}^{-1} C_V^*(P) e^{(\frac{\Delta E_f}{kT})} \quad (5)$$

0-7803-6279-9/00/$10.00 © 2000 IEEE

where g_{bc} is the geometric factor, $C^*_I(P)$ and $C^*_V(P)$ are the pressure dependent equilibrium concentration of interstitials and vacancies, k is the Boltzman's constant and T is the absolute temperature. Pressure due to loops is calculated using the lattice mismatch techniques described in [10]. ΔE_f is the change in the defect formation energy due to the self-force of a dislocation loop during the emission and absorption process at its edge [11].

$$\Delta E_f = -\frac{\mu b \Omega}{4\pi(1-\nu)R}\ln\left(\frac{8R}{r_c}\right) \tag{6}$$

where μ is the shear modulus, b is the magnitude of the Burgers vector of the loop, Ω is the atomic volume of Si, ν is the Poisson's ratio, r_c is the core (torus) radius of the loop, and R is the radius of the dislocation loop.

The density of dislocation loops decreases during oxidation and annealing in an inert ambient while their average radius increases. The capture or emission rate of interstitials bounded by the dislocation is proportional to the rates of emission and absorption of point defects at the loop boundaries and given as:

$$\frac{dN_{all}}{dt} = K_I \int_{0^+}^{\infty} (C_I - C_{Ib}) f_D(R)dR - K_V \int_{0^+}^{\infty} (C_V - C_{Vb}) f_D(R)dR \Bigg|_{\text{at the boundary}} \tag{7}$$

where K_I is the reaction rate between interstitials and dislocation loops. K_V is a similar reaction rate between vacancies and dislocation loops. They both are the function of the loop radius and the diffusivity of interstials and vacancies respectively. C_I and C_V are the concentration of interstitials and vacancies. The capture rate is also modulated by a log normal distribution function in order to count the effects of all loops. Equation (7) becomes positive during oxidation since oxidation injects interstitials and increases the excess interstitial amount in the bulk. It is obvious that total density of the interstitials inside the loops increases. The quantity in (7) will be negative below certain value of R at some temperatures during annealing in an inert ambient and the density of intertitials inside the loops will decrease (dissolution of loops).

It can be said that two different processes affect the growth of the average dislocation loop radius, Rp. Interstitials injected to the bulk during oxidation contribute to the growth of the large loops. Loop-to-loop interactions, with the large loops growing at the expense of smaller ones (Ostwald ripening), contribute to the growth of the large loops during annealing in an inert ambient. These processes can be expressed by an empirical formula that is similar to [6]:

$$\frac{dR_p}{dt} = K_{Rp}\frac{C_I}{C_{Ib}} \tag{8}$$

where K_{Rp} is a constant. It is clear that the average radius growth rate will be higher during oxidation and will be lower during annealing in an inert ambient.

Further reduction in the number of equations can be achieved by using statistical information about the loops.

$$\frac{R_{p\max}}{R_p} = 2.7 \tag{9}$$

$$R_{p\max} = R_p + 5\sigma \tag{10}$$

where R_{pmax} is the radius of the biggest loop. Equation (9) comes from [4] and derived from transmission electron microscopy (TEM) experiments. Assuming (10) is meaningful when compared to TEM data. This allows us to calculate Dall using (3). Thus, we only need to solve a two-moment problem, (7) and (8).

In order to take into account the effects of dislocation loops on the interstial concentration, the interstial continuity equation needs to be modified by adding a new flux as follows:

$$\frac{dC_I}{dt} = \nabla\left[D_I C_I^*(P)\nabla\left(\frac{C_I}{C_I^*(P)}\right)\right] - K_R(C_I C_V - C_I^*(P)C_V^*(P)) - K_I\int_{0^+}^{\infty}(C_I - C_{Ib})f_D(R)dR \tag{11}$$

where K_R is the bulk combination rate. The reaction rate now includes the pressure term, as well. The flux due to loop to interstitial interaction is the same as the one in (7). The vacancy continuity equation needs to be derived in an expression similar to (11).

SIMULATIONS

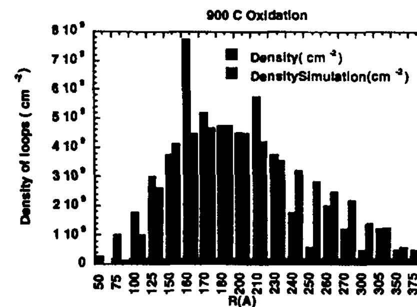

Fig.1. Log normal distribution of data [4] and simulation result.

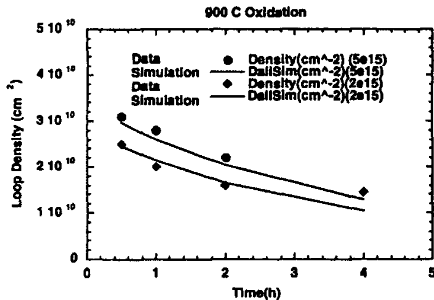

Fig.2. Variation in total loop density as a function of annealing time. Data from [4]

It should be noted that data from [4,12,15] are used to calibrate the loop model and data from [13,14] are used to verify the loop model. The model is implemented in Florida Object Oriented Process Simulator (FLOOPS).

Fig. 1, shows the log normal distribution of the loop density for oxidation data [4] and the simulation for a 900°C, 30 minutes dry oxygen anneal. A Log normal distribution follows the data nicely. Similar results were obtained for other annealing times also.

The variation of the loop density with time for two different implant doses is shown in Fig. 2. It can be seen that the loop density decreases with time. Simulation (solid lines) shows some discrepancy at larger annealing times but it is in excellent agreement with experiments for shorter annealing times. As the annealing time increased loops start forming networks and statistical interpretation of TEM pictures gets harder.

Fig. 3, shows the experimental data and the simulation fits to the increase in the average loop radius with time upon annealing under an inert ambient at different temperatures. As seen from the experimental data and the simulations, the growth rate of the loops is proportional to the anneal temperature. The average loop radius increases with the annealing time. The increase is very small at the low temperatures but it is higher for high annealing temperatures.

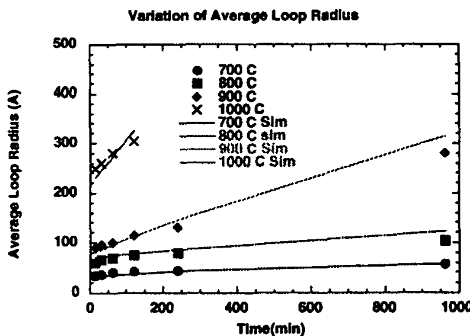

Fig.3. Variation of average loop radius as a function annealing time. Data from [12,15]

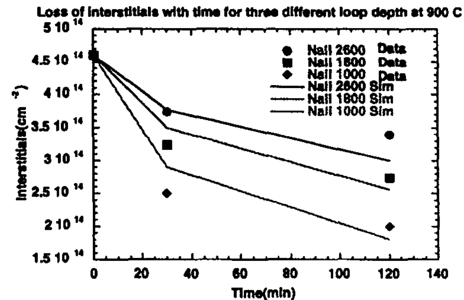

Fig.4. Loss of interstitials with time for three different loop depth at 900°C. Data from [13]

Fig. 1-3, show a good agreement between the calibration data and simulations.

After calibrating the loop model with the same fitting parameters for the oxidation and the inert anneal data, the model is used to simulate the loop dissolution and the interstitial loss as a function of time at three different loop depths from the surface. This is shown in Fig. 4. First, Si^+ was implanted into silicon at 30 keV and 50 keV and dose of 1e15cm^{-2} to produce EOR dislocation loops. The initial loop depth was 2600 A. Second, chemical mechanical polishing (CMP) technique was used to vary the loop depth to 1800 A and 1000 A. Third, samples are annealed at 900°C for 30 minutes and 120 minutes and at 1000°C for 15 minutes and 30 minutes. Experimental details can be found in [13]. Loops are expected to be in coarsening / dissolution mode at 900°C and in dissolution mode at 1000°C. Fig. 4 shows that as the loop layer gets closer to the surface, the loss of interstitials increases due to surface recombination. The rate of loss decreases after 30 minutes of annealing. Simulation verified these results.

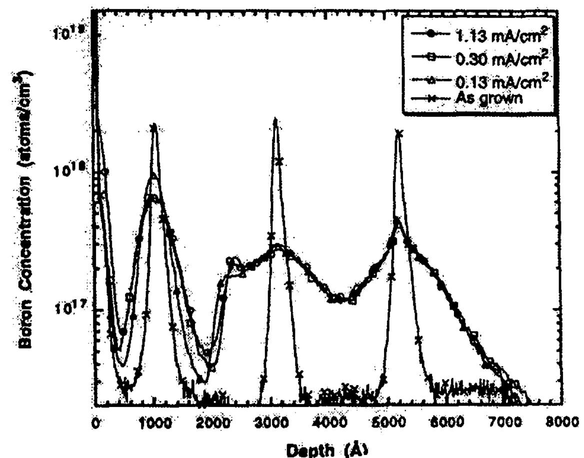

Fig.5. SIMS profiles of Boron spikes after Si^+ implantation at different dose rates and annealing at 800°C for 3 minutes.

The model is also used to study the effects of dislocation loops on boron diffusion. Experimental details are explained in [14] and can be summarized as follows: Boron doping superlattices (DSLs) were grown in silicon. A series of Si^+ implants of 30 and 112 keV at a dose of 1e15cm^{-2} was carried out to amorphize these DSLs. This placed the a/c interface between first and second spikes. The dose rates of implants are varied. Post implantation anneals were done in a rapid thermal annealing furnace at 800°C for 5 seconds and 3 minutes. It is shown that the implantation dose rate affects the interstitial release from EOR implant damage region in silicon (e.g. loop density changes). Therefore, the diffusion enhancement of boron changes. Fig. 5, is from [14] and shows the secondary ion mass spectrometry (SIMS) profiles of boron spikes after Si^+ implantation at different dose rates and annealing at 800°C for 3 minutes. As the dose rate increases (loop density changes), the amount of interstitial flux into the regrown region increases, as well.

The simulation results of boron profiles, annealed at 800°C for 3 minutes, with two different loop densities are shown in Fig. 6, along with the as implanted profile. It is assumed that EOR point defect profile does not change. Since the implantation generated {311}s as well as dislocation loops at the EOR region in this experiment, {311}s were simply modeled by an exponential decay in this simulation. Simulations correctly predict the diffusion enhancement in both below and above the a/c interface. The change in the diffusion enhancement rate of the first peek due to dose rate change is not as significant as the experimental data.

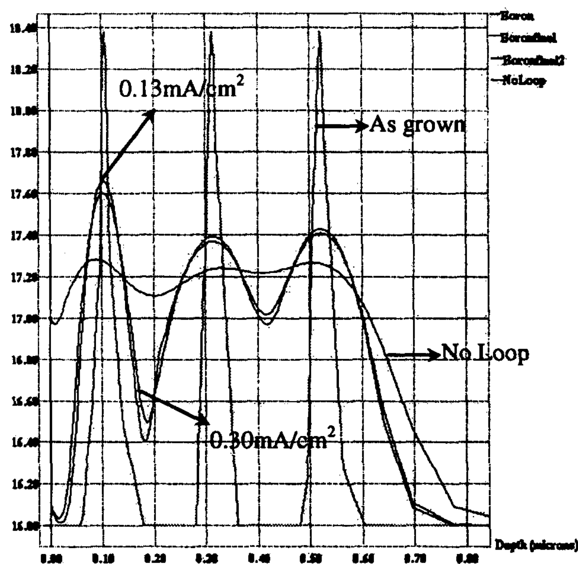

Fig.6. Boron profiles with 2 different loop density and no loop layer, annealed at 800°C for 3 min.

This might be due to the fact that the {311} model used is very simple and there is no interaction between loops and {311}s in the model. Fig. 6 also shows a profile with no loop layer. In this case, {311} defects and excess interstitials below a/c interface exist but there are no loops. The diffusivity enhancement of all boron spikes increases dramatically. It is very clear that dislocation loops are efficient sinks for interstitials.

CONCLUSIONS

A single statistical point defect based model for the evolution of dislocation loops during oxidation and annealing under an inert ambient is developed. The model assumes that the radius and the density of the dislocation loops follow a log normal distribution. The developed model correctly predicts the density of loops and the average radius of the loops and the number of interstitials captured by the loops. It also agrees with the depth dependence of the data. Its effects on the dopant diffusion are very clear.

ACKNOWLEDGMENT

The authors would like to thank SRC for their support.

REFERENCES

[1] M. Servidori, Nucl. Instrum. Methods Phys. Res. B. 19/20, 443 (1987)
[2] K. S. Jones, S. Prussin, and E. R. Weber. Appl. Phys. A 45,1 (1998)
[3] P. M. Fahey, S. R. Mader, S. R. Stiffler, R. L. Mohler, J. D. Mis, J. A. Slinkman. IBM Journal of research and development 36/2, (1992)
[4] H. Park, K. S. Jones and M. E. Law. J. electrochem. Soc. 141, 759 (1994)
[5] H. L. Meng, S. Prussin, M. E. Law and K. S. Jones. J. Appl. Phys. 73,2 (1993)
[6] C. Bonafos, D. Mathiot, A. Claverie. J. Appl. Phys. 83,16 (1998)
[7] J. Lothe and J. P. Hirth, J. Appl. Phys., 38, 845 (1967)
[8] L. Borucki, Workshop on Numerical Modeling of Processes and Device for integrated circuits: NUPAD IV, Seattle WA (1992)
[9] J. P. Hirth and J. Lothe, Theory of Dislocations, pp 497-516, Wiley, NY (1982)
[10] H. Rueda and M. E. Law, MSM 98, Santa Clara, CA
[11] S. D. Gavazza and D. M. Barnett, J. Mech. Phys. Solids 24, 171 (1976)
[12] S. Chaudhry, J. Liu, K.S. Jones and M. E. Law. Solid State Electronics 38,7 (1995)
[13] R. Raman, M. E. Law, V. Krishnamoorthy, K.S. Jones, and S. B. Herner. Appl. Phys. L. 74,11 (1999)
[14] L. S. Robertson, A. Lilak, M.E. Law, K. S. Jones, P. S. Kringhoj, L. M. Robin, J. Jackson, P. S. Simons, and P. Chi. Appl. Phys. L. 71,21 (1997)
[15] J. Liu, M. E. Law and K.S. Jones. Solid State Electronics 38,7 (1995)